EXPERIMENTAL AND ANALYTICAL METHODS FOR THERMAL INFRARED SPECTROSCOPY OF COMPLEX DUST COATINGS IN A SIMULATED ASTEROID ENVIRONMENT. C. R. Tinker[1], T. D. Glotch[1], L. Breitenfeld[1], and L. Li[1], [1]Stony Brook University Center for Planetary Exploration (Connor.Tinker@Stonybrook.edu).

Introduction: Fine particles are common across airless body surfaces and often manifest as surficial coatings with the potential to modify the spectral signatures of underlying substrates. This can make accurate spectral analysis of surface materials challenging, especially for thermal infrared (TIR) techniques for which the spectral properties concurrently depend on grain size and albedo. Further complexity is presented when these coatings occur as discontinuous patterns in which some substrate is exposed, and some is masked. Discontinuous patterns are distinguished by scale as having macroscopic or microscopic discontinuity, with the former being patches of homogeneous covering portions of the substrate and the latter being randomly distributed individual particles on the substrate. Investigations of asteroid (101955) Bennu's surface by NASA's Origins, Spectral Interpretation, Resource Identification, and Security-Regolith Explorer (OSIRIS-REx) have revealed contradictions between spectral and thermophysical results that we hypothesize to indicate the presence of thin and/or laterally discontinuous dust coatings. The spectral and thermophysical effects of thin-continuous, macro-discontinuous, and micro-discontinuous dust cover are not well understood and require relevant laboratory analyses to be deconvolved in an orbital setting. We have constructed a custom environment chamber that enables the controlled deposition of size-regulated dust particles in coatings with varying continuity and thickness. TIR spectra of coated substrates acquired in a Simulated Asteroid Environment (SAE) are used to investigate the extent to which dust coatings of different thicknesses and arrangements contribute to orbital spectral signatures of airless body surfaces.

Motivation: Measurements from the OSIRIS-REx Thermal Emission Spectrometer (OTES) show that the lowest thermal inertia values across Bennu's surface are associated with the largest boulders, while regions lacking boulders have a higher than average thermal inertia [1-4]. [3] proposed that the low thermal inertia of Bennu's boulders may be explained by local dust cover, which is supported by the association of transparency features in thermal infrared (TIR) spectra attributable to dust with regions dominated by rough, dark boulders [2-3,5-7]. This is contradicted by thermal model results that can provide accurate fits to the OTES data while assuming a constant thermal inertia with depth [1-2], and additional models show continuous dust layers as thin as 10 – 100 μm can distort diurnal temperature curves in a way that is inconsistent with the OTES results [8]. However, thin and heterogeneous dust coatings could contribute to a lower thermal inertia of boulders without significantly distorting diurnal temperature curves in the manner discussed by [8]. Dust-free thermal models of Bennu fit best with OTES data, however thin dust coatings (<50 μm) with low spatial coverage (5 – 10%) cannot be ruled out as they produce an acceptable fit to the observations. So, while very thin coatings may be present, their deposition pattern and thickness would need to be verified through laboratory studies with samples of known material and thermal properties. There is no fully relevant laboratory study that has characterized the spectral and thermophysical effects of dust across a variety of coating thicknesses and patterns.

Deposition Chamber and Dust Characterization: The dust deposition chamber built in this study uses elements from previous methods to enable accurate and repeatable dust coatings up to 1000 μm thick [9-17]. The chamber and its five subsystems are shown in Figure 1 and described in detail in [18]. Physical parameters of the dust coating structure have strong effects on TIR spectra due to scattering [19], changes in overall albedo [20], and increased obscuration [13]. Dust coating thickness is estimated using a WiTEC confocal microscope as an average of 50 measurements of the difference in Z stage positions for the focus point of the closest exposed substrate and top of the dust layer. Spatial coverage for micro-discontinuous and macro-discontinuous coatings are measured optically through a pixel count of stitched microscope images. Coating porosity is constrained by weighing the sample and sample cup before and after deposition then calculating volume from the average coating thickness and assuming the density of antigorite (2.5 g/cm^3).

Sample Preparation: For this work, both the substrate and dust are sourced from antigorite, the dominant analog mineral used in mixtures simulating complex CI and CM analog mixtures used to simulate Bennu's spectra [21-23]. Based on [20-22] nanophase carbon lamp black is mixed with the dust to achieve a visible albedo consistent with Bennu (~0.04) [20,24]. Coarse particulate substrates (180-250 μm) were created by wet and dry sieving hand ground antigorite then washing with ethanol to remove clinging fines. Coarse particulates were also baked at 500°C for 24 hours to remove hydration features. Chip substrates

were cut, sanded, and polished to fit the sample cup and provide a smooth reference surface. Examples of coated samples with varying continuity and thickness are shown in Figure 2.

Analysis: TIR (5-50 µm) spectra of each sample are acquired under SAE conditions using the Planetary and Asteroid Regolith Spectroscopy Environmental Chamber (PARSEC) at Stony Brook University [25]. PARSEC was modeled after the chamber described in [26] to measure samples under environmental conditions typical of airless bodies. PARSEC is connected to a Nicolet 6700 FTIR spectrometer equipped with a cesium iodide (CsI) beamsplitter and a deuterated L-alanine doped triglycine sulfate (DLaTGS) detector with a CsI window.

Several spectra were acquired for a variety of experimental extremes to establish baseline and threshold capabilities of the dust deposition chamber. Consistent with previous studies under SAE conditions, the chips exhibited the highest contrast while the particulates had the lowest [27]. Compared to uncoated counterparts, chips with discontinuous coatings <50 µm thick resulted in lower overall contrast, increased emissivity longward of the Christensen feature (CF), and a reduced silicate roll-off shortward of the CF. A chip continuously coated with the maximum 1mm of dust exhibited similar spectral features to the dust alone with some differences in slope occurring between ~1000 and 700 cm^{-1}. More samples with closer matching porosities will be required to determine if these differences are induced by substrate emission or differences in the dust structure.

References: [1] Rozitis B. et al. (2019) *Asteroid Sci.,* 2189, 2055. [2] Rozitis B. et al. (2020) *Sci. Adv.,* 6, eabc3699. [3] DellaGiustina D. N. et al. (2019) *Nature Astro*., 3, 341-351. [4] Lauretta D. S. et al. (2019) *Nature,* 568, 55-60. [5] Hamilton V. E. et al. (2021) *Astro. & Astro.,* 650, A120. [6] Hamilton V. E. et al. (2019) *Asteroid Sci.,* 2189, 2044. [7] DellaGiustina D. N. et al. (2020) *Science*, 370, 674. [8] Biele J. et al. (2019) *Prog. Earth & Planetary Sci.,* 6, 48. [9] Crisp J. and Bartholomew M. J. (1992) *JGR*, 97, 14691-14699. [10] Fischer E. M. & Pieters C. M. (1993) *Icarus*, 102(2), 185–202. [11] Singer R. B. & Roush T. L. (1983) *LPSC XIV*, 708–709. [12] Johnson J. R. & Grundy W. M. (2001) *Geophysical Research Letters*, 28(10), 2101–2104. [13] Johnson J. R. et al. (2002) JGR Planets, 107, 5053. [14] Rivera-Hernandez F. et al. (2015) *Icarus*, 262, 173–186. [15] Wells E. N. et al. (1984) *Icarus*, 58(3), 331–338. [16] Graff T. G. et al. (2001) LPSC, #1899. [17] Graff T. G. (2003) M. S. Thesis, 106 pp., ASU, Tempe, AZ. [18] Tinker et al. (2022) LPSC, #1960 [19] Salisbury J. W. & Wald A. (1992) *Icarus*, 96(1), 121–128. [20] Breitenfeld L. B. et al. (2019) *LPSC*, #1866. [21] Breitenfeld L. B. et al. (2020) *LPSC*, #1124. [22] Breitenfeld L. B. et al. (2021) *JGR Planets*, 126(12), e2021JE007035. [23] Howard K. T. et al. (2011) *Geochimica et Cosmochimica Acta*, 75(10), 2735–2751. [24] Clark B. E. et al. (2011) *Icarus*, 216(2), 462–475. [25] Shirley K. A. and Glotch T. D. (2019) *JGR Planets*, 124, 970-988. [26] Thomas I. R. et al. (2012) *Rev. Sci. Instr.*, 83(12). [27] Glotch T. D. et al. (2018) *JGR*, 123, 2467-2484.

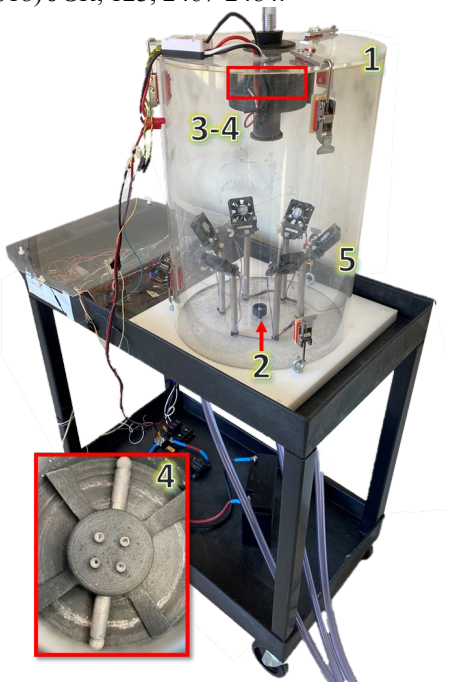

Figure 1: Dust deposition chamber designed and used for this study. Image outlined in red shows an internal view of the agitation basket. Subsystems are: Enclosure (1), Sample Holder (2), Agitation Basket (3), Agitator (4), Lofting Fans (5).

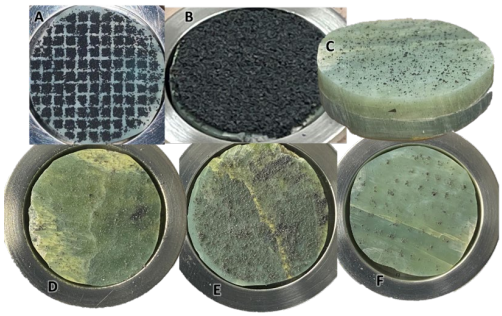

Figure 2: Chip substrates with various coatings: (A) Max Thickness Macro-Discontinuous, (B) Max Thickness Continuous, (C) Visible Micro-Discontinuous, (D) Opaque Micro-Discont., (E) Dense Micro-Discont., and (F) Min. Macro-Discontinuous.